Environmental Technology & Innovation 27 (2022) 102765

Contents lists available at ScienceDirect

Environmental Technology & Innovation

journal homepage: www.elsevier.com/locate/eti

Clay honeycomb monoliths for the simultaneous retention of lead and cadmium in water

Mohammadi Ahrouch [a,b], José Manuel Gatica [a,c,*], Khalid Draoui [b], Dolores Bellido-Milla [c,d], Hilario Vidal [a,c]

[a] Departamento de Ciencia de los Materiales e Ingeniería Metalúrgica y Química Inorgánica, Universidad de Cádiz, Puerto Real, Spain
[b] Laboratoire Matériaux et Systemes Interfaciaux LMSI, FS, Université Abdelmalek Essaadi, Tetouan, Morocco
[c] IMEYMAT, Instituto Universitario de Investigación en Microscopía Electrónica y Materiales, Universidad de Cádiz, Puerto Real, Spain
[d] Departamento de Química Analítica, Universidad de Cádiz, Puerto Real, Spain

ARTICLE INFO

Article history:
Received 11 April 2022
Received in revised form 30 May 2022
Accepted 16 June 2022
Available online 23 June 2022

Keywords:
Cadmium
Lead
Clay
Co-adsorption
Honeycomb monoliths

ABSTRACT

Natural illite–smectite and stevensite Moroccan clays were used for the simultaneous removal of lead and cadmium from aqueous medium. The clays were employed in raw state and extruded as honeycomb monoliths form without any additives, which confirms the novelty of this approach in water treatment. The experiments were done in batch conditions with continuous stirring and using a recirculated flow, respectively. In addition to a characterization of the clays by XRF, XRD, TGA, laser granulometry, N_2 physisorption, FTIR spectroscopy, SEM-EDS and evaluation of the cation exchange capacity, special attention was paid to the influence on the co-adsorption of variables such as adsorbent dosage, contact time and initial concentration of Cd^{2+} and Pb^{2+}. Pseudo-second order kinetics and good fitting to Redlich–Peterson model for both heavy metals were found. Our results also suggest that Pb^{2+} and Cd^{2+} uptake is controlled by chemisorption with predominance of Langmuir characteristics. No significant depletion of the metals retention attributable to competition was observed, particularly for the stevensite (maximum retention capacity of 1.2 mg Pb^{2+}/g and 4.6 mg Cd^{2+}/g) that showed higher specific surface area. For both clays, cadmium ions adsorption was relatively favoured in the bimetallic solution, and the honeycombs kept the powders performance. Honeycomb monoliths as a compact adsorbent offer a promising way of water treatment thanks to their stability and easy incorporation into dynamic processes avoiding the issues of pressure drop under wastewater circulation.

© 2022 The Author(s). Published by Elsevier B.V. This is an open access article under the CC BY-NC-ND license (http://creativecommons.org/licenses/by-nc-nd/4.0/).

1. Introduction

Direct or indirect release into the environment of wastewaters containing heavy metals has continued growing in the last decades due to the development of industrial activities such as those related to metal plating, mining, tanneries, fertilizers synthesis, batteries, paper manufacture, pesticides, etc. (Chen et al., 2023; Parveen et al., 2022; Zhang et al., 2022). Contrary to organic pollutants, heavy metals are not biodegradable, so they tend to accumulate in living organisms,

* Corresponding author at: Departamento de Ciencia de los Materiales e Ingeniería Metalúrgica y Química Inorgánica, Universidad de Cádiz, Puerto Real, Spain.
E-mail address: josemanuel.gatica@uca.es (J.M. Gatica).

https://doi.org/10.1016/j.eti.2022.102765
2352-1864/© 2022 The Author(s). Published by Elsevier B.V. This is an open access article under the CC BY-NC-ND license (http://creativecommons.org/licenses/by-nc-nd/4.0/).

being toxic or carcinogenic (Aziz et al., 2022; Singh et al., 2022). Among the heavy metals, cadmium and lead are placed on the top of the Substance Priority List of Agency Toxic Substances and Disease Registry (ATSDR). In fact, Cd have been categorized as "Group 1" (carcinogenic to humans) while Pb compounds are grouped as "Group 2A" (probably carcinogen to humans) by the International Agency for Research on Cancer and, in addition, they cause multiple disorders in animals and plants (Kumar et al., 2022). The maximum concentration levels permitted in drinking water (Joseph et al., 2019) for cadmium are 0.005 mg L^{-1} according to the United States Environmental Protection Agency (USEPA) and 0.003 mg L^{-1} for the World Health Organization (WHO). In the case of lead these limits are 0.0 mg L^{-1} for the USEPA and 0.01 mg L^{-1} for the WHO. Cadmium is also the most toxic heavy metal found in the industrial effluent. It plays a major role in the industries like plating, cadmium–nickel battery, phosphate fertilizers, stabilizers and alloys. On the other hand, the main cause of the association of Pb in the industrial effluent is mainly due to lead–acid battery wastewater and often appears in wastewater from electroplating, electrical and steel industries, explosive manufacture, etc. (Femina Carolin et al., 2017). These highly toxic metals are generated from industrial processes in massive quantity and disposed of into the water canals and tributaries of the river devoid of proper treatment (Kumar et al., 2022).

Ionic exchange and adsorption are among the most used methods to retain heavy metals because they are cheap and highly efficient (Di et al., 2022; Fu and Wang, 2011), although they also exhibit shortcomings, reason by which many other alternatives like filtration membranes for example (Sharma et al., 2022) are being explored. In the case of ionic exchange, synthetic resins are the preferred materials (Alyüz and Veli, 2009; Liu et al., 2011), their retention capacity depending on variables such as pH, temperature, initial metal concentration and contact time (Gode and Pehlivan, 2006). Though the option of natural zeolites has been also tested (Motsi et al., 2009; Ostroski et al., 2009; Taffarel and Rubio, 2009), their use is still very limited to lab scale. In the case of adsorption, although there are emerging materials such as ordered mesoporous carbons (Gang et al., 2021) and biochars (Amalina et al., 2022) within the wide family of carbonaceous adsorbents, conventional active carbons (Jusoh et al., 2007; Kang et al., 2008) are still the most employed materials by far, but they are relatively expensive and difficult to regenerate. Thus the research of new low cost and easily available adsorbents has become a priority (Bailey et al., 1999; Barakat, 2011; Lee and Choi, 2018; Sanchooli et al., 2016; Siddiqui, 2018).

In the above context, literature dealing with the use of clays, either in their raw state or after modification, to remove heavy metals has greatly developed as well illustrated not only by single research papers (Abdellaoui et al., 2019; Abu-Danso et al., 2020; Ayari et al., 2005; Baker, 2009; Khalfa et al., 2021; Mnasri-Ghnimi and Frini-Srasra, 2019) but also reviews (Arif et al., 2021; Novikau and Lujaniene, 2022; Otunola and Ololade, 2020; Uddin, 2017; Zhang et al., 2021). However, it is surprising that related works employing structured adsorbents are still scarce, especially those reporting on honeycomb monoliths (García-Carvajal et al., 2019), in spite of the fact that clays are in general easily extrudable (Gatica and Vidal, 2011), and considering the intrinsic advantages of this design for environmental processes (Cybulski and Moulijn, 1994). As well known, honeycomb monoliths are continuous unitary structures that contain a large number of straight, identical, parallel channels, equally accessible to the contact with the flow. This configuration confers a high geometric area per unit of volume, easy scaling up, low-pressure drop, and high resistance to clogging in effluents. In the case of natural clays, one of the most interesting properties of these structured filters is their easier handling when they are in contact with water, as they allow their extraction from the aqueous media after the adsorption process (García-Carvajal et al., 2019).

In recent papers we demonstrated that some honeycomb monoliths prepared integrally from different natural clays were very efficient to eliminate methylene blue (Ahrouch et al., 2019a; Gatica et al., 2013) and lead from aqueous solutions (Ahrouch et al., 2019b). Subsequently, we demonstrated that some of the above mentioned natural clays extruded as honeycomb monoliths were similarly capable to retain cadmium from water (Ahrouch et al., 2020).

The objective of this work is to take a step forward in this research by evaluating the behaviour of the clay monoliths that are the focus of our study when both metals, Pb and Cd, are present. On one hand, this scenario would approach in a better way the environmental conditions. On the other hand, it would be interesting to elucidate whether their coexistence in the aqueous media has a negative effect on the adsorbent response due to the metals competition or there is some selectivity in the adsorption. Although many authors already investigated the simultaneous adsorption of different metallic ions by clay-based materials (Padilla-Ortega et al., 2013; Vhahangwele and Mugera, 2015), and specifically that of Pb^{2+} and Cd^{2+} (Adebowale et al., 2006; Djukić et al., 2013; He et al., 2018; Jiang et al., 2010; Sellaoui et al., 2018; Zhu et al., 2021), to our knowledge this co-adsorption was not studied yet with honeycomb-shaped adsorbents. Therefore, special attention will be paid here to the comparison between powdered and structured adsorbent materials.

2. Materials and methods

2.1. Raw materials and honeycomb monoliths preparation

Two natural clays sampled in deposits located at the north of Morocco were used: an illite–smectite (called I-S) and a stevensite (called ST). These clays were selected because they had shown very promising performance in the adsorption of Pb^{2+} and Cd^{2+}, respectively, in previous studies (Ahrouch et al., 2019b, 2020). It is worth noting that clay materials are considered low-cost adsorbents in the field of water treatment (Joseph et al., 2019). To illustrate this idea, the price of a bentonite may range from 0.05 to 0.2 U$/kg while the average price of a commercial activated carbon is 0.8–1.1 U$/kg (De Gisi et al., 2016).

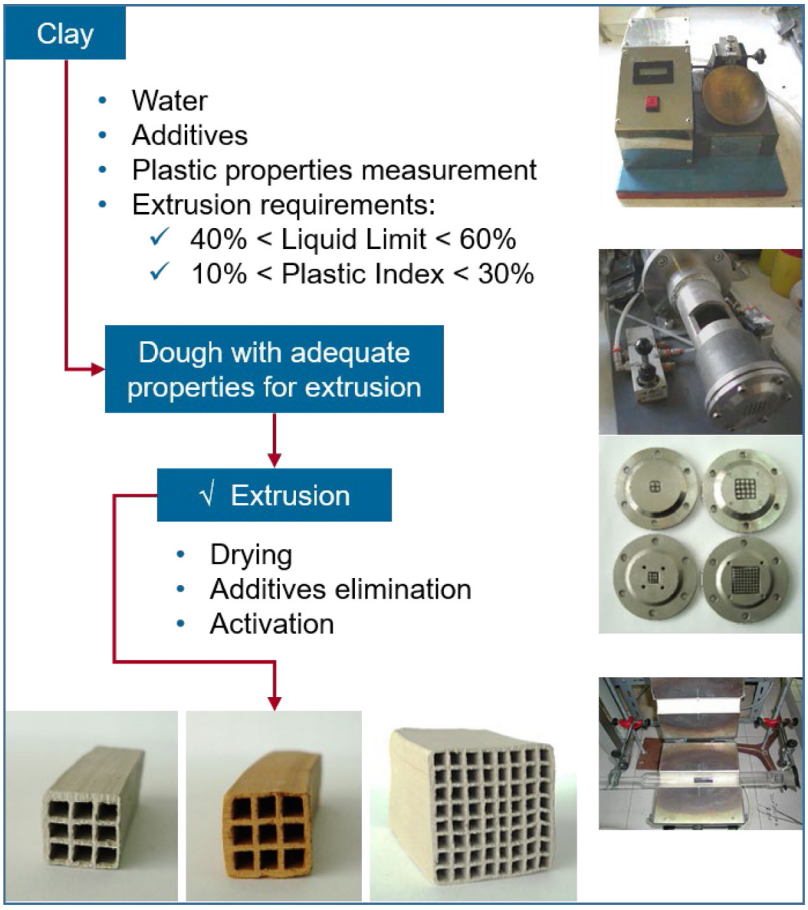

Fig. 1. Scheme of the general procedure followed to prepare clay honeycomb monoliths. In this work no additives were necessary for the extrusion so preventing the additive elimination step. Pictures of the liquid limit Casagrande device, pneumatic extrusion machine, extrusion dies and experimental set up for the activation step employed in this study are also included.

The fabrication of the honeycomb monoliths from the clay powders was possible without additives, except water, and was carried out through extrusion following Casagrande's methodology to predict the extrudibility of the corresponding pastes (Gatica et al., 2004). After drying the monoliths overnight at 60 °C, they were subjected to a calcination treatment at 400 °C (4 h) and 450 °C (5 h) for the ST and I-S samples, respectively, in order to make the materials waterproof according to the methodology previously reported (Cifredo et al., 2010). Previous results have proved the durability of the clay honeycombs in aqueous medium in experiments up to 16 h long (Ahrouch et al., 2019b). Fig. 1 shows a schematic of the clay honeycomb monoliths preparation followed according to the above description. In this particular work, the resulting monoliths, 4–5 cm long, had circular section with 1.4 cm diameter, approximately 50 cells/cm^2, 0.33 mm of wall thickness and 72% of open frontal area (Fig. 2a).

2.2. Adsorbents characterization

The chemical analysis of the clays by X-ray fluorescence (XRF) was performed in a Bruker S4 Pioneer spectrometer, while their Cation Exchange Capacity (CEC) was measured through the hexamine cobalt (III) trichloride method (Cieseielski et al., 1997). In the particular case of the clay monoliths, a complementary study by XRF in multipoint mode was carried out to analyse the elemental composition in 1.5 mm × 0.5 mm rectangular zones of the monolith walls in order to check the homogeneity of the main clay elements distribution. This special XRF analysis was also applied to selected clay monoliths submitted to adsorption studies.

The textural characterization of monoliths pieces was carried out by means of N_2 physisorption at −196 °C using an Autosorb IQ (QuantaChrome), first degassing the clay samples at 150 °C for 2 h. The obtained isotherms were used to estimate BET surface area (S_{BET}) and total pore volume data.

Fourier Transform Infrared (FTIR) spectra were recorded in a Thermo Vertex 70 spectrophotometer, using KBr pellets which contained 1 mg of clay diluted per 200 mg of mixture. The measurements were performed in absorbance mode operating in the 4000–400 cm^{-1} range with 4 cm^{-1} resolution.

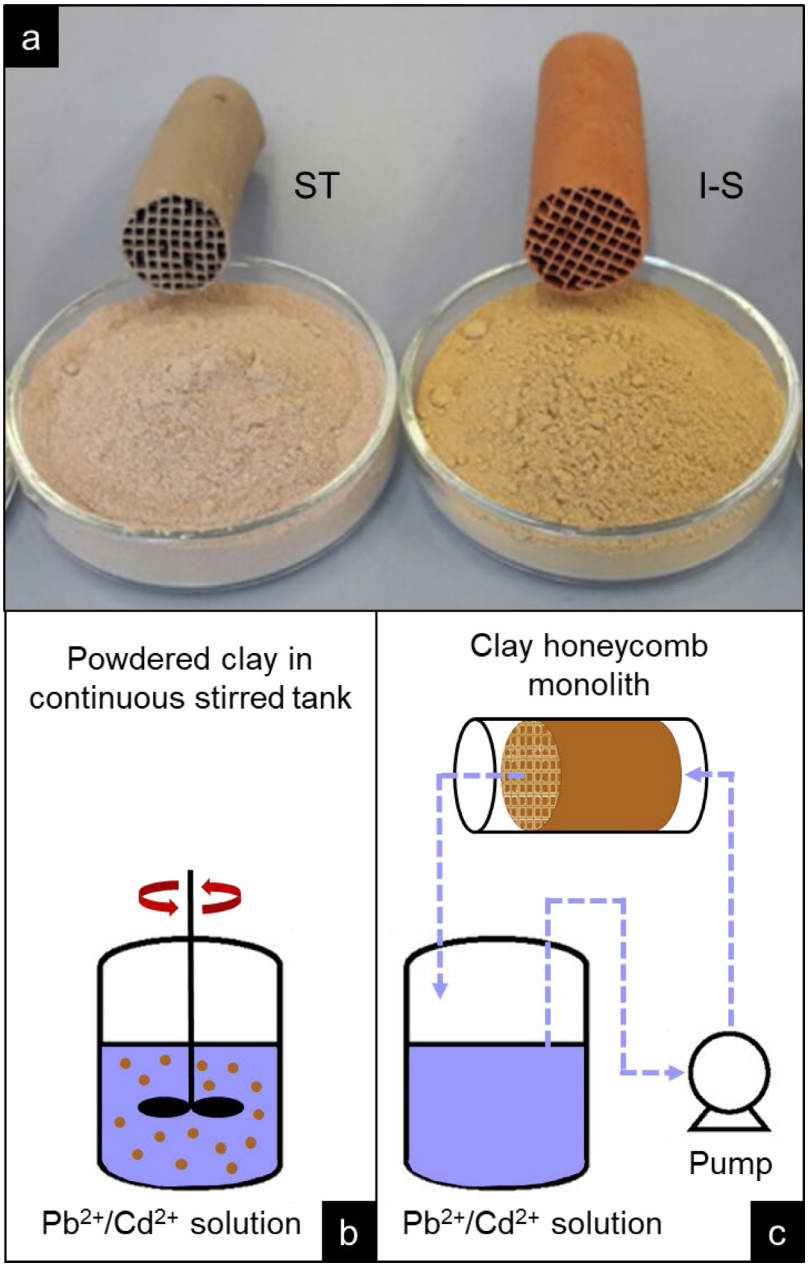

Fig. 2. Integral honeycomb monoliths prepared from the studied clays along with their respective starting powders (a) and experimental setup for the tests of retention of Pb^{2+} and Cd^{2+} using the clays in the form of powder (b) and clay honeycomb monoliths (c).

The thermogravimetric analysis (TGA) was carried out in a Shimadzu T-50 thermobalance, using 50 mg of sample and a heating rate of 10 °C/min.

Scanning Electron Microscopy (SEM) images were acquired in a FEG Nova NanoSEM 450 microscope operating at 30 kV.

X-ray diffraction (XRD) analyses were performed at room temperature on a Bruker D8 Advance A25 powder diffractometer operating with Cu K_α radiation and LINXEYE detector. The 2θ angle ranged from 1.5° to 75°, with scanning steps of 0.017° and a counting time per step of 8 s.

Finally, the granulometric study was carried out using a Malvern Mastersizer 2000 granulometer, operating with laser diffraction and by previously applying ultrasound to the samples in deionized water for 5 min. The results were obtained in each case from the average of three measurements to ensure reproducibility.

2.3. Adsorption tests

The co-adsorption tests over the powdered clay samples were performed at room temperature in batch mode (continuous stirring at 150 rpm) using aqueous solutions (40 mL) of Pb^{2+} and Cd^{2+} nitrates, with initial concentrations ranging from 2 to 150 ppm (Fig. 2b). In all cases the pH was fitted to 4.5 with the help of an acetic/acetate buffer after seeing in previous studies that this value was the optimal for the adsorption of both lead (Ahrouch et al., 2019b) and cadmium (Ahrouch et al., 2020), and representative of environmental conditions. First, we studied the influence of the clay amount which was changed between 0.025 g and 12.000 g, adjusting the lead and cadmium concentrations to 30 ppm and 2 ppm, respectively, and after 12 h of contact. These concentration values were the same as those previously used in single metals adsorption studies (Ahrouch et al., 2019b, 2020). Thus, the adsorbed amount (q_e) of both metal ions at a certain time and at co-adsorption equilibrium, as well as the removal percentage were determined using the following equations:

$$q_e = \frac{(C_0 - C_e) \times V}{m} \tag{1}$$

$$\%\ Removal = \frac{(C_0 - C_t)}{C_0} \times 100 \tag{2}$$

where C_0 is the initial concentration of metal ions (mg L^{-1}); C_t and C_e are the concentration of metals (mg L^{-1}) at a certain time and at equilibrium, respectively; V is the volume of solution (L), and m is the adsorbent mass (g).

Once fixed the minimum amount of clay needed to remove simultaneously and significantly the same percentage of the initial Pb^{2+} and Cd^{2+}, we studied the kinetics of the process by monitoring the evolution of the amount adsorbed as function of the contact time (up to 240 min). The experimental data were fitted to three mathematical models (pseudo-first order: PFO, pseudo-second order: PSO, and Elovich) that are usually employed to analyse the adsorption kinetics of heavy metal ions onto clay-based adsorbents (Ajala et al., 2022). The nonlinear shape of these three models mentioned above can be expressed as shown in Eqs. (3), (4), and (5), respectively.

$$q_t = q_e.(1 - exp^{-k_1 t}) \tag{3}$$

$$q_t = \frac{k_2.q_e^2.t}{1 + k_2.q_e.t} \tag{4}$$

$$q_t = \frac{1}{\beta} \ln(1 + \alpha.\beta.t) \tag{5}$$

where q_t and q_e are the amount adsorbed (mg g^{-1}) of metal ion at a certain time and at co-adsorption equilibrium, respectively; k_1 (min^{-1}) is the rate constant of PFO model, k_2 (g mg^{-1} min^{-1}) is the rate constant of PSO model; α (mg g^{-1} min^{-1}) is the initial adsorption rate constant; β (g mg^{-1}) is Elovich constant, which is related to the extent of surface coverage and the activation energy associated with chemisorption data. Besides that, the kinetic study and their suitability in the experimental data format provide information about the adsorption mechanism.

Finally, fixed the saturation time, clay amount and pH, we studied the influence of the initial concentration of both heavy metals. The experimental data obtained were fitted to three of the most used isotherm models (Langmuir, Freundlich and Redlich–Peterson) (Baker, 2009; Chabani et al., 2009). As a novelty respect to our previous studies (Ahrouch et al., 2019b, 2020), nonlinear regression was followed for this fitting because it is a more adequate method that can be used to estimate models' parameters, and it can be applied even if the isotherm model cannot be linearized (Nagy et al., 2017). So, the nonlinear forms of the mentioned models of adsorption isotherms are described by Eqs. (6), (7), and (8), respectively:

$$q_e = \frac{Q_m.K_L.C_e}{1 + K_L.C_e} \tag{6}$$

$$q_e = K_F.C^{\frac{1}{n}_F}{}_e \tag{7}$$

$$q_e = \frac{K_{RP}.C_e}{1 + a_{RP}.C_e^g} \tag{8}$$

where q_e (mg g^{-1}) is the adsorption capacity at equilibrium; C_e (mg L^{-1}) is the equilibrium concentration of metals; Q_m (mg g^{-1}) is the maximum monolayer coverage capacity; K_L (L mg^{-1}) is the Langmuir model constant; K_F ((mg g^{-1}).(L $mg^{-1})^{1/n_F}$) is the Freundlich model constant; n_F is the Freundlich intensity parameter; K_{RP}(L g^{-1}) and a_{RP}(mg^{-1}) are the Redlich–Peterson model constants; g is the Redlich–Peterson exponent.

Indeed, the fitness of adsorption isotherms can contribute substantially to elucidating adsorption mechanisms. In this sense, the Langmuir model assumes that the surface is energetically uniform and the adsorption is limited to monolayer. This model is generally suitable for describing the chemisorption mechanism. Whereas, Freundlich model is based on the heterogeneity of adsorbent surface. Adsorption primarily concerns the most energetic sites. This model is suitable for both monolayer and multilayer adsorptions. Finally, the Redlich–Peterson equation is widely used as a compromise between Langmuir and Freundlich systems.

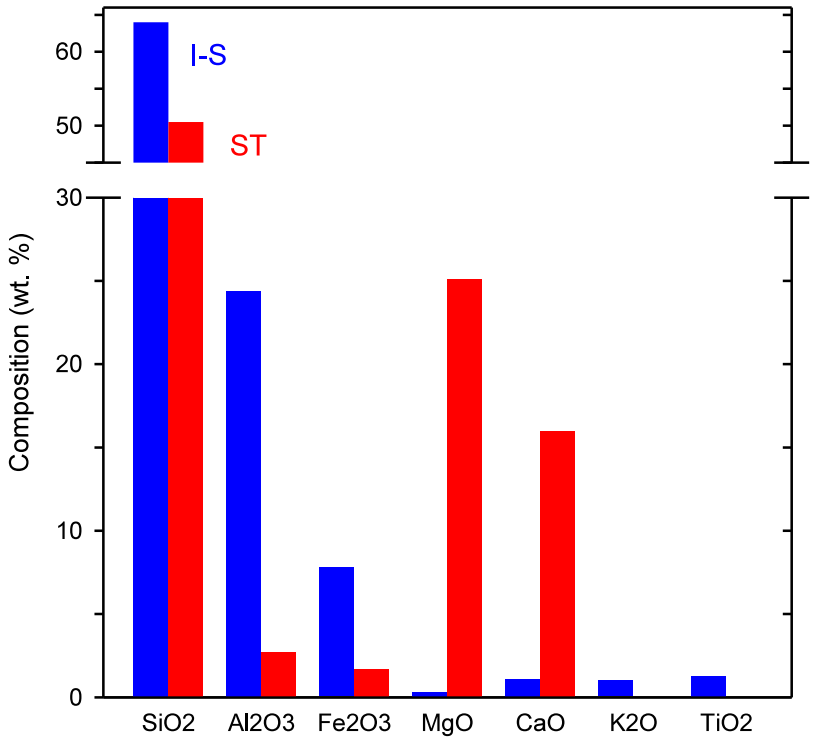

Fig. 3. Compositional analysis of the clay honeycombs as obtained by means of XRF.

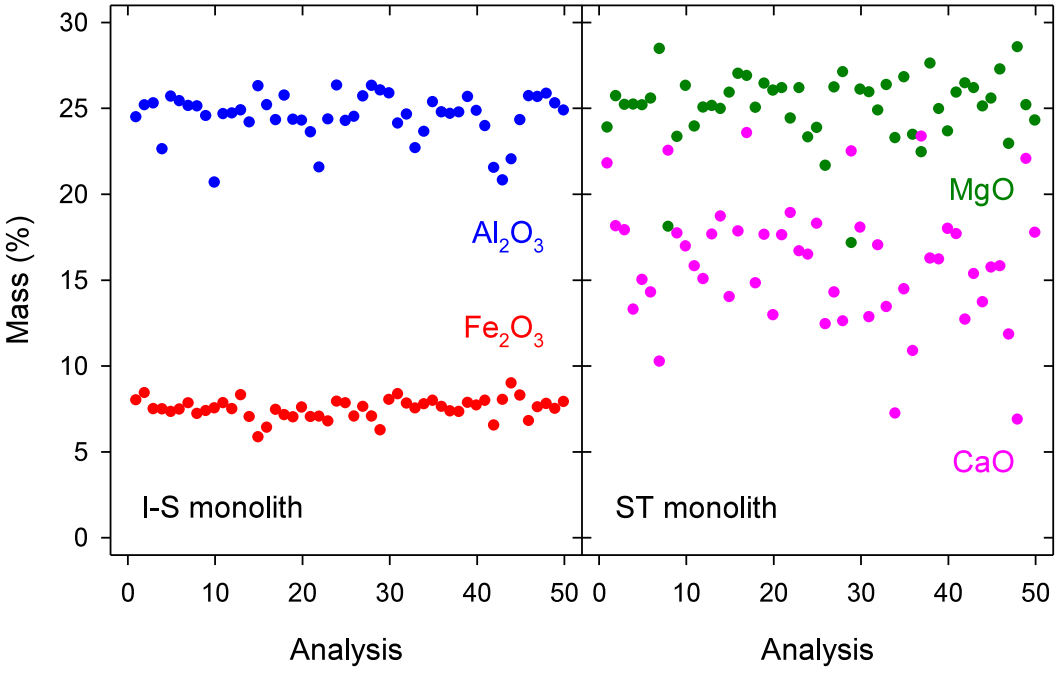

Fig. 4. Elemental composition obtained by XRF multipoint mode analysis over 1.5 mm × 0.5 mm rectangular zones of the clay honeycomb monoliths. The mean average composition for this study resulted to be 24.4 wt% and 7.9 wt% for Al_2O_3 and Fe_2O_3, respectively, in the case of I-S, and 25.1 wt% and 16.0 wt% for MgO and CaO, respectively, in the case of ST.

We applied a convenient Excel-based user interface to provide a useful tool for solving the nonlinear method to fit kinetic and equilibrium data, along with Origin Pro-2018 software for calculating the model and statistical parameters.

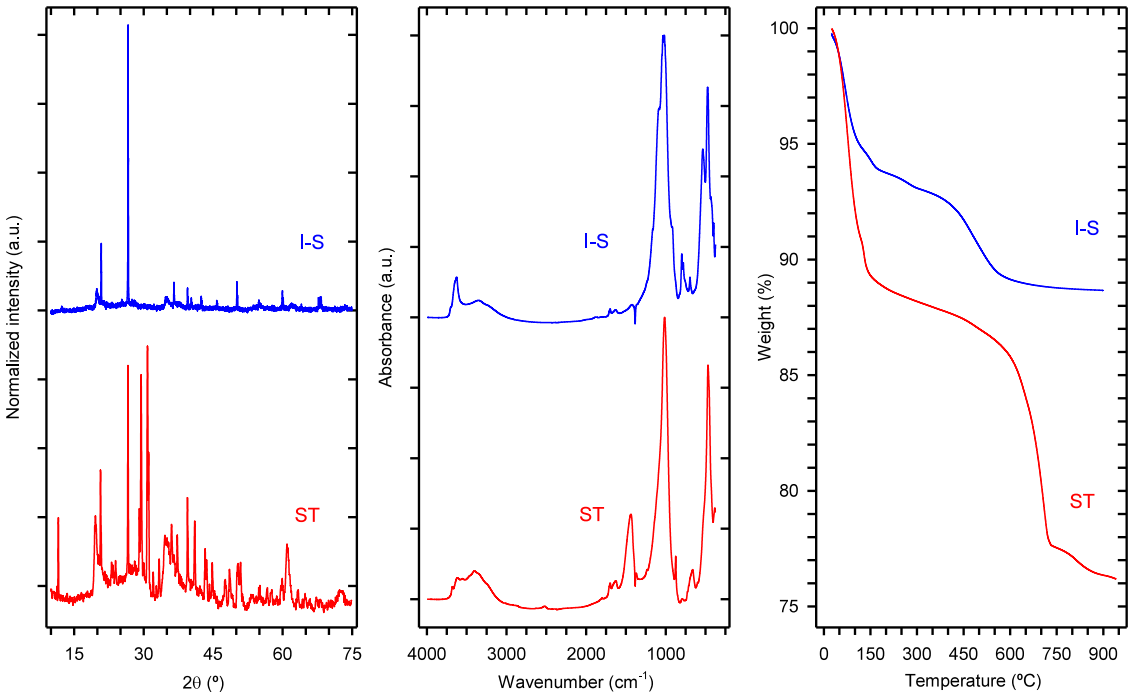

Fig. 5. Results for the I-S and ST clays obtained by means of XRD (left), FTIR spectroscopy (centre) and TGA (right) techniques.

To study the retention of lead and cadmium by the honeycomb monoliths we employed approx. 5 g weighted samples and a 1200 mL/min recirculating flow of the solution (1 L) containing Pb^{2+} and Cd^{2+} (2–150 ppm) with the help of a centrifugal pump (Fig. 2c).

In all cases, after the experiments, the solutions were centrifuged at 5000 rpm for 15 min, being further filtered with a 0.45 μm pore size Nylon membrane. The determination of the residual lead and cadmium in the solutions was carried out by atomic absorption spectroscopy using an air–acetylene flame in a Thermo Scientific ICE 3000 (AA series) spectrometer. All measurements were made with the main wavelengths of lead and cadmium, 217 nm and 228.8 nm, respectively. The calibration curves were built with the standards corresponding to the linear range of each element using an acetic acid–acetate buffer solution at pH 4.5 as solvent.

3. Results and discussion

3.1. Physico-chemical characterization of the clays

Fig. 3 summarizes the results of the chemical analysis of the clay honeycombs by means of XRF. Notice the higher content of Fe in the I-S clay, which explains its reddish colour (Fig. 2a), and the higher content of Mg and Ca in the ST clay, typical of a stevensite mineral. The complementary multipoint mode analysis of the honeycomb walls performed at the millimetre level not only confirmed the above observations and the average values shown in Fig. 3, but also showed the relative distribution of the most distinctive elements (see Fig. 4). In this sense, notice the higher heterogeneity of the ST clay monolith.

FTIR spectra and XRD diagrams (Fig. 5) showed a good agreement with this chemical analysis. They were dominated by the characteristic peaks of quartz (ICCD database PDF code = 65-0466), and in the case of the ST clay revealed an additional infrared band at 1450 cm^{-1} attributable to carbonates as well as XRD peaks which could be assigned to dolomite, ankerite and gypsum (PDF codes = 12-0088, 34-0517 and 21-0816, respectively). The more complex mineralogy of this sample might explain the higher fluctuation of Mg and Ca content in the ST clay monolith shown in Fig. 4. The TGA curves, which served to select the final calcination treatment of the clays indicated in the experimental section and are included in Fig. 5, were also consistent with the clays mineralogical composition. They exhibited a small weight loss above 700 °C for the ST sample that was related to carbonates decomposition.

Fig. 6 collects the main data derived from the N_2 physisorption study of the clay monoliths. Like the CEC (63 and 55 meq/100 g for I-S and ST, respectively) the S_{BET} values were in the order of the most common clay minerals (Humphrey and Boyd, 2011). Notice however the higher BET surface area (106.8 vs 39.6 m^2/g) and porosity (0.093 vs. 0.079 cm^3/g) of the ST monolith compared to the I-S monolith. These values slightly decreased in the final honeycomb monoliths with

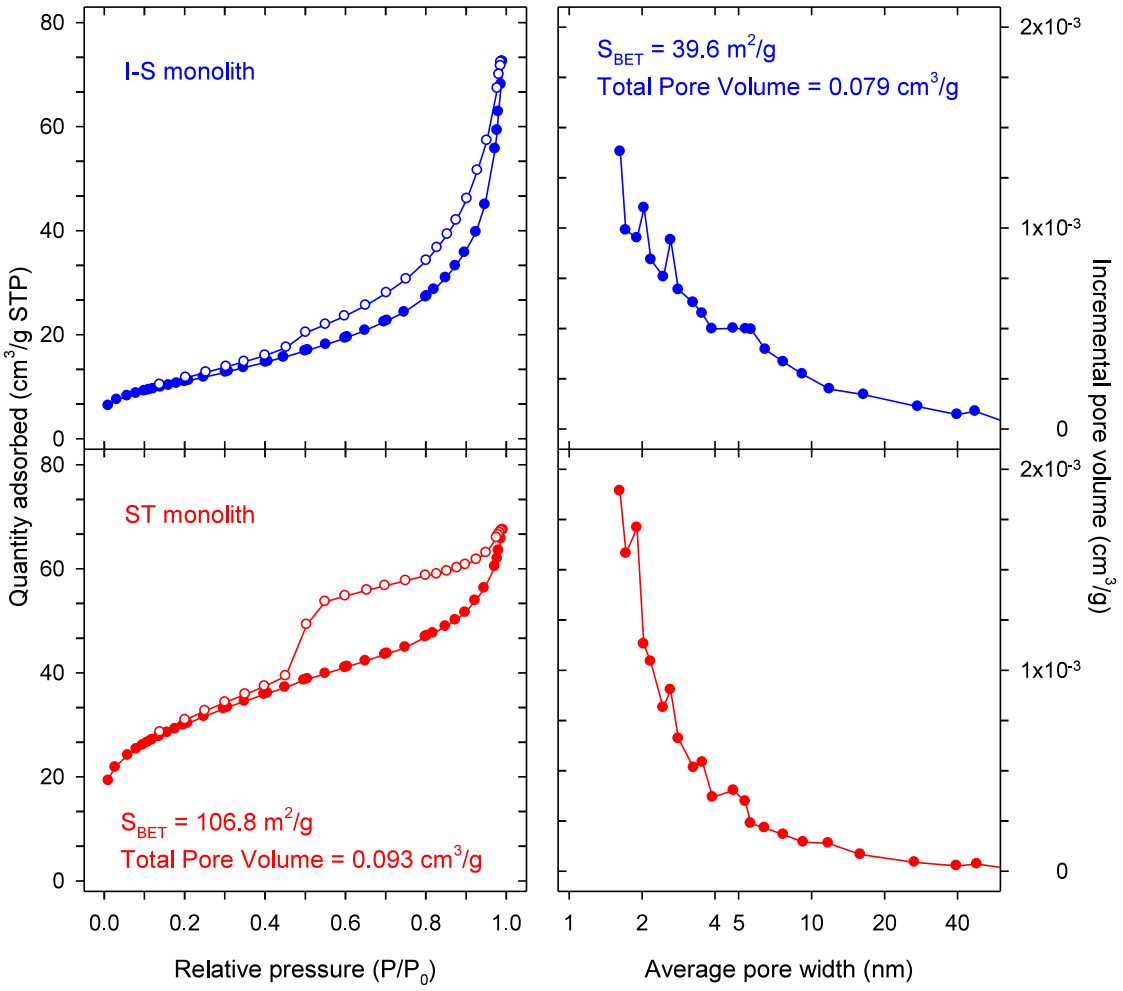

Fig. 6. Results for the I-S and ST clay monoliths obtained by means of N_2 physisorption. Isotherms showing the adsorption (●) and desorption (○) branches and pore size distributions are displayed on the left and right, respectively. Results of the BET specific surface area and total pore volume data are also shown.

respect to the starting powders (Ahrouch et al., 2019b), as a consequence of the applied calcination treatment, although the shape of the isotherms did not change, being II-type, typical of mainly macroporous adsorbents, according to the IUPAC classification (Thommes et al., 2015). It is however worth noting the difference in the hysteresis loop between the two clay samples investigated. Whereas the I-S monolith exhibited a H3-type one, denotative of aggregates of plate-like particles frequently found in clay materials, the loop of the ST monolith was of H4-type, often found with aggregated crystals of solid materials (Thommes et al., 2015).

Images obtained by SEM for the monolithic samples (Fig. 7) showed that our clays are predominantly composed of an agglomerate of particles with heterogeneous size and irregular form which give them a look very similar to that previously observed for other smectite-type natural clays (Chafik et al., 2009; Cifredo et al., 2010; Harti et al., 2007). Previous complementary EDS analysis of the clays here investigated but in the form of powders (Ahrouch et al., 2019b, 2020) provided results in good agreement with those obtained for the massive analysis by XRF (Fig. 3).

Finally, the study of the clays through laser granulometry led to particle size distribution curves having maxima at 3 and 8 μm for I-S and ST, respectively, and with similar shape to those obtained in previous studies with other clays which could be also extruded without additives (Vidal et al., 2016).

Summarizing, in this work we deal with two natural clays that are clearly different not only from the mineralogical point of view (illite–smectite *vs* stevensite), which is reflected in different structure and chemical composition (high Fe and Al *vs* Mg and Ca content, respectively), but also according to their granulometry and texture (threefold surface area for the ST).

Table 1
Parameters obtained in the non-linear regression fitting of the experimental data of the uptake kinetics at 25 °C onto the clay powders.

Sample	I-S		ST	
Metal ions	Pb^{2+}	Cd^{2+}	Pb^{2+}	Cd^{2+}
Pseudo-first-order				
$Q_{e,1}$	1.070	0.028	0.796	0.109
K_1	1.651	1.431	0.501	0.137
R^2_{adj}	0.987	0.980	0.967	0.934
χ^2	0.012	0.0005	0.034	0.026
SSE	0.012	$1.36\ 10^{-5}$	0.023	0.001
SD	0.035	0.0011	0.048	0.010
BIC	−77.92	−159.28	−70.12	−107.74
Pseudo-second-order				
$Q_{e,2}$	1.091	0.029	0.834	0.117
K_2	3.778	114.98	0.937	1.694
R^2_{adj}	0.999	0.996	0.981	0.983
χ^2	0.001	0.0001	0.029	0.006
SSE	0.001	$2.56\ 10^{-6}$	0.013	0.0003
SD	0.010	0.0005	0.036	0.005
BIC	−107.74	−179.35	−76.96	−122.19
Elovich model				
α	$2.57\ 10^{11}$	$3.67\ 10^{8}$	45.73	0.09
β	31.21	$1.07\ 10^{3}$	13.14	56.49
R^2_{adj}	0.992	0.978	0.910	0.979
χ^2	0.0081	0.0006	0.115	0.005
SSE	0.0082	$1.52\ 10^{-5}$	0.063	0.0003
SD	0.028	0.0012	0.079	0.005
BIC	−82.79	−157.98	−58.02	−122.19

3.2. Adsorptive performance

Fig. 8 shows the effect of the amount of clay used in the form of powder on the simultaneous retention of Pb^{2+} and Cd^{2+}. This kind of experiment allowed defining the amount of clay for the kinetic study, which resulted to be 0.3 and 0.4 g for the I-S and ST samples, respectively. These values were taken as the minimum ones that approximately allow simultaneous non-negligible and similar attenuation of the initial Pb^{2+} and Cd^{2+}, around 20% and 30% for I-S and ST, respectively.

The effect of the contact time using the above cited powder amounts can be observed in Fig. 9. Notice how in general the co-adsorption is very fast in both clays, mainly occurring in the first 10 min. In any case, for the rest of the study we selected 150 min because this is the time in which it seems that a plateau is reached for this type of curves in both clays.

The analysis of the kinetic results using PFO, PSO and Elovich models led to the fittings that are also included in Fig. 9 and the corresponding parameters reported in Table 1. Furthermore, according to the Montecarlo approach recommended for an adequate estimate of the validity of nonlinear models (Spiess and Neumeyer, 2010), in addition to the conventional R^2 evaluation, the chi-square test (χ^2) was performed to determine the degree of difference between the experimental data and the model-computed data, which is determined by the following formula:

$$\sum \frac{(q_e^{exp} - q_e^{cal})^2}{q_e^{cal}} \tag{9}$$

where q_e^{cal} (mg g^{-1}) is the experimental adsorption capacity at equilibrium obtained from formula (1); q_e^{cal}(mg g^{-1}) is the model-calculated adsorption capacity at equilibrium. Then, a smaller value for χ^2 suggests a better fitting model. Likewise, in order to further validate the suitability of the kinetic and adsorption isotherms to the experimental adsorption data, as well as to confirm the best-fit model, adjusted R^2 coefficient (R^2_{adj}), residual sum of squares (SSE), standard deviation of residues (SD), and Bayesian information criterion (BIC) were estimated using the following formulas (Spiess and Neumeyer, 2010):

$$R^2_{adj} = 1 - \left(1 - R^2\right) \cdot \left(\frac{n-1}{n-p-1}\right) \tag{10}$$

$$SSE = \sum (q_e^{exp} - q_e^{cal})^2 \tag{11}$$

$$SD = \sqrt{\left(\frac{1}{n-p}\right) \cdot \sum (q_e^{exp} - q_e^{cal})^2} \tag{12}$$

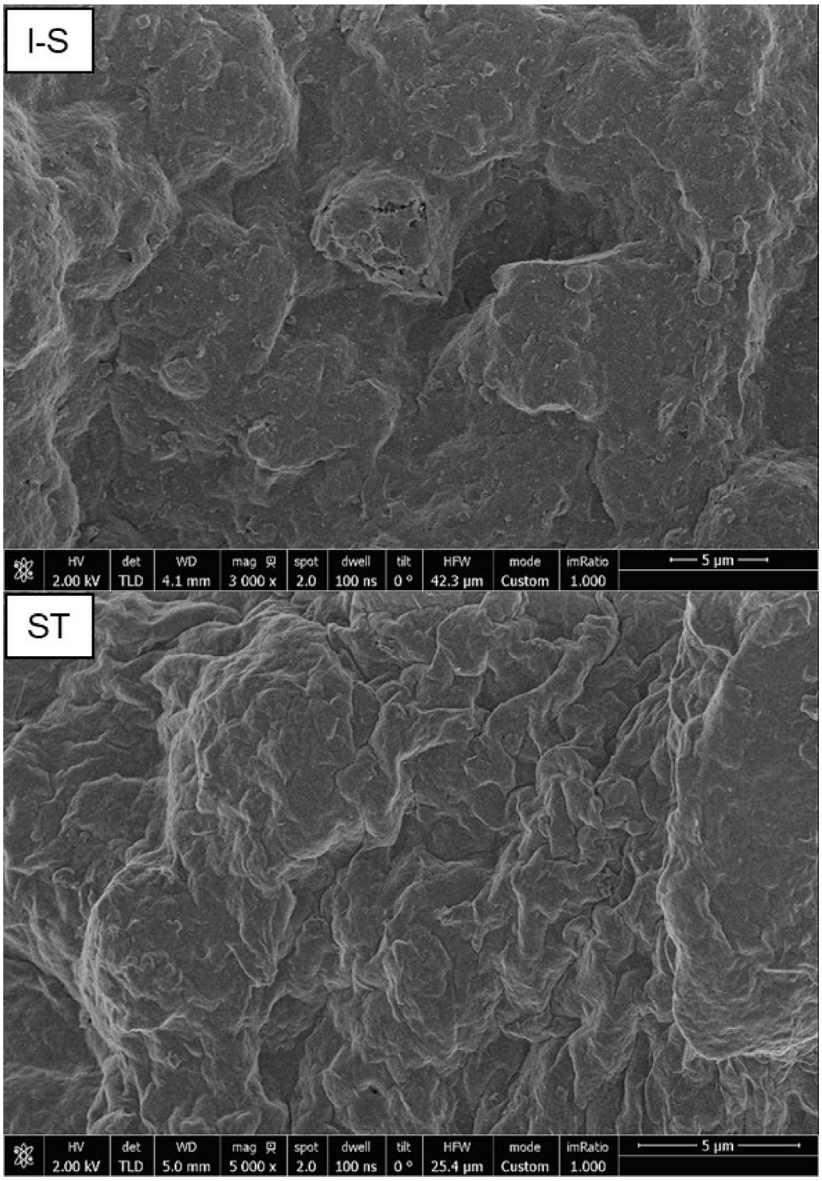

Fig. 7. SEM images of the studied clay monoliths.

$$BIC = nln\left(\frac{SSE}{n}\right) + pln\,(n) \tag{13}$$

where n is the number of data points, and p is the number of parameters in the fitting model. Besides the lowest χ^2 value, the lower the values of SD and BIC parameters, and the closer to 1.000 the R^2_{adj} value, the better fitting of the applied model.

With independence of the clay and metal considered, taking into account all the above mentioned parameters, the best fitting of the experimental data was obtained for a PSO model, in good agreement with the results obtained in previous studies dealing with individual adsorption of Pb^{2+} (Ahrouch et al., 2019b) and Cd^{2+} (Ahrouch et al., 2020). This is a first indication that the adsorption process can be chemically controlled. In any case, Elovich's equation is more used to describe chemisorption processes (Ajala et al., 2022), so we also employed it for our analysis. In this sense, the values of the corresponding α parameter for the adsorption of Pb^{2+} and Cd^{2+} on both I-S and ST clays resulted to be of the same order of magnitude as those reported in the literature for the adsorption of both metal ions onto the MMA-Na-Y-Zeolite adsorbent (Elwakeela et al., 2017). Moreover, the values of β were consistent with the levels reported by El-Korashy et al. in the adsorption of Pb^{2+} on the bentonite/thiourea–formaldehyde composite surface (El-Korashy et al., 2016). Both observations confirm that the uptake of Pb^{2+} and Cd^{2+} on our clays is controlled by chemisorption.

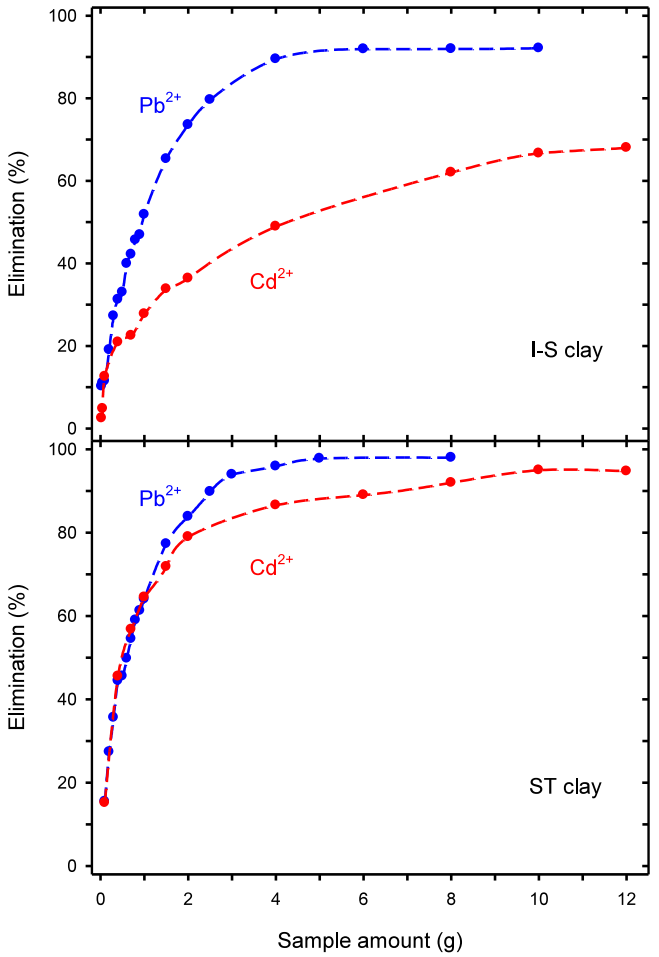

Fig. 8. Retention of Pb^{2+} and Cd^{2+} as function of the amount of clay used in the form of powder. Initial concentration: 30 ppm of Pb^{2+} and 2 ppm of Cd^{2+}. pH: 4.5. Contact time: 12 h.

In order to fully evaluate the co-adsorption performance of the two clay minerals as adsorbents for the removal of Pb^{2+} and Cd^{2+}, adsorption isotherms of both metal ions were also determined experimentally at room temperature and pH 4.5. Fig. 10 shows the adsorption isotherms of the two studied clays obtained by varying the initial concentration of lead and cadmium in the range up to 150 ppm. As it can be observed, the I-S clay is better to retain lead while the ST clay removes a higher amount of cadmium. The same behaviour was found in our studies working with both metals separately. Our results are also consistent with observations made by other authors (Ayari et al., 2005; Baker, 2009) who found that clay minerals belonging to the smectite group exhibit higher selectivity for Pb^{2+}, which was related to the sorption of Pb hydroxycomplexes (Ayari et al., 2005; Sajidu et al., 2008).

These experimental data were also non-linearly fitted (see Fig. 10) to well-known isotherm models such as Langmuir, Freundlich and Redlich–Peterson (Nagy et al., 2017). We found that the best result was obtained for the latter, especially considering the χ^2 data. In any case, the goodness of this fitting was very similar to that of Langmuir which was the proposed model in previous studies with individual adsorption. In fact, the values obtained for the g parameter in the fitting to the Redlich–Peterson model (Table 2), which are relatively closer to 1 than those reported by other authors (Chabani et al., 2009), combined with the values of the a parameter which are not $\gg 1$ (requisite to transform Redlich–Peterson isotherm into Freundlich isotherm (Tran et al., 2017)) suggest the predominance of the Langmuir characteristics on the metals' adsorption (Liu et al., 2011). For this reason, we took the Qm value of the Langmuir model to estimate the maximum retention capacity of our clays, which resulted to be 1.5 and 1.2 mg/g for Pb^{2+} and Cd^{2+}, respectively, in the case of the I-S clay, and of 1.2 and 4.6 mg/g for the ST. Certainly, these amounts are lower than those reported by Sellaoui et al. in a similar recent study (Sellaoui et al., 2018), but in that work the authors employed a bentonite–chitosan composite made through a complex elaboration in which additionally the clay was previously purified using hydrogen peroxide solution, being subsequently activated using sulphuric acid solution. Adebowale et al. also reported higher capacity for the simultaneous adsorption of lead and cadmium onto a kaolinite clay, but in that study the raw material was also

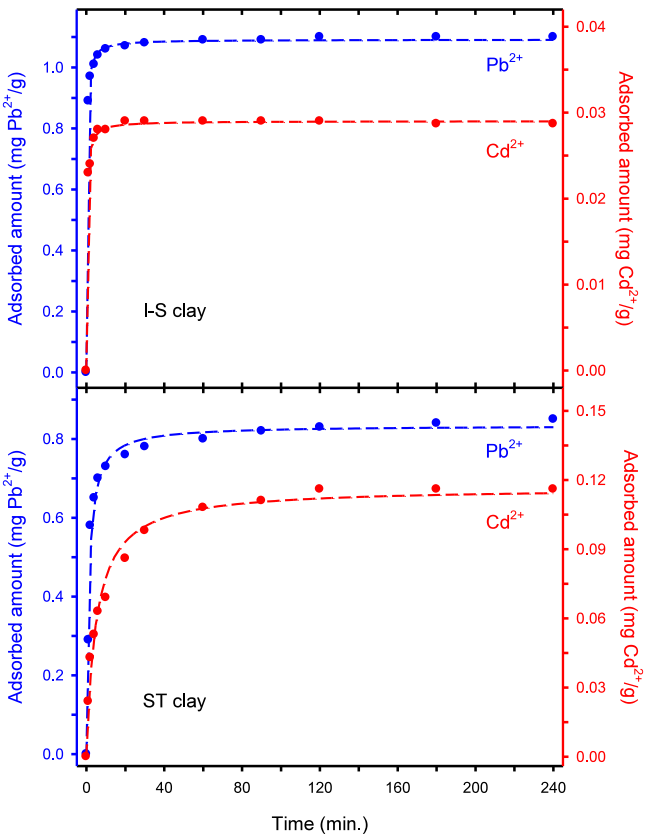

Fig. 9. Retention of Pb^{2+} and Cd^{2+} by the clays in the form of powder as function of the contact time. Initial concentration: 30 ppm of Pb^{2+} and 2 ppm of Cd^{2+}. pH: 4.5. Clay amount: 0.3 g of I-S and 0.4 g of ST. Fitting of the experimental data to the Pseudo-Second Order kinetic model is also included in each case.

subjected to a time and reactants-consuming purification process which we avoided intentionally to minimize adsorbent production costs (Adebowale et al., 2006). In the same way, although some synthetic mineral adsorbents exhibited higher adsorption capacity of both metal ions pollutants than natural clays, their synthesis methods are more complex and costly compared to the studied clay materials (Chen and Shi, 2017).

Fig. 11 shows the result of the co-adsorption experiments over the I-S and ST clay honeycomb monoliths. As it can be seen, the use of this design does not significantly change, from a qualitative point of view, the adsorptive performance of the clay powders (compare with Fig. 10), with a relative preference of I-S for lead and ST for cadmium. In the case of the monoliths, we also performed a non-linear fitting of the isotherms to the Langmuir, Freundlich and Redlich–Peterson models (Table 3), leading to similar conclusions as those derived from the powders analysis. On the other hand, comparison with the powders in terms of retention capacity (mg/g) indicates that this remains almost the same for the ST monolith while it is even slightly improved in the case of the I-S monolith, with the shared advantage that no polluted sludge is generated. Moreover, let us recall that the monolithic filters once saturated by lead and cadmium, being unitary structures, can be handled more easily, with lower impact onto the environment, and even with chance of recycling if needed for other use.

In our opinion, it is even more interesting to compare the adsorbents performance with respect to that they exhibited in a mono-solute system, i.e. water containing just one metal (Ahrouch et al., 2019b, 2020). In this sense, as shown in Fig. 12, we observed that in both clays the coexistence of Pb^{2+} and Cd^{2+} in aqueous solution only diminishes slightly the capacity to retain lead, more in the case of the I-S sample which exhibited a maximum capacity of 2.5 mg/g of Pb^{2+} when this cation was alone (Ahrouch et al., 2019b). On the contrary, the binary system (Pb^{2+}/Cd^{2+}) hardly affects the retention of cadmium, which keeps being practically the same or even slightly improves when compared to the scenario in which this metal is alone (Ahrouch et al., 2020). This suggests a certain preference in the co-adsorption versus the cadmium. On the other hand, the sum of Pb^{2+} and Cd^{2+} retained amounts was higher than any of the amounts retained in the experiments with separate metals. This suggests that either the metals do not compete for the same adsorption sites or new available centres are activated when the clays face a bi-solute system. This result contrasts with the above mentioned references (Adebowale et al., 2006; Sellaoui et al., 2018) which reported that adsorption of one metal ion is suppressed to some degree by the other, i.e. the adsorption capacities decreased in binary systems due to an antagonistic

Table 2
Parameters obtained in the non-linear regression fitting of the experimental data of the adsorption isotherms at 25 °C onto the clay powders.

Sample	I-S		ST	
Metal ions	Pb^{2+}	Cd^{2+}	Pb^{2+}	Cd^{2+}
Langmuir model				
Q_m	1.53	1.21	1.23	4.58
K_L	0.056	0.013	0.087	0.016
R^2_{adj}	0.999	0.989	0.994	0.992
χ^2	0.002	0.007	0.006	0.027
SSE	0.001	0.004	0.004	0.046
SD	0.022	0.036	0.038	0.123
BIC	−37.34	−32.43	−31.96	−20.22
Freundlich model				
n_F	3.07	1.81	3.82	1.75
K_F	0.286	0.053	0.331	0.202
R^2_{adj}	0.977	0.993	0.942	0.996
χ^2	0.038	0.009	0.065	0.028
SSE	0.026	0.002	0.044	0.022
SD	0.093	0.029	0.121	0.086
BIC	−23.08	−34.80	−20.44	−23.87
Redlich–Peterson model				
K_{RP}	0.099	0.033	0.085	0.156
a_{RP}	0.088	0.223	0.043	0.305
g	0.94	0.62	1.10	0.59
R^2_{adj}	0.999	0.993	0.997	0.997
χ^2	0.0005	0.008	0.002	0.012
SSE	0.0006	0.002	0.002	0.014
SD	0.018	0.034	0.032	0.084
BIC	−39.76	−33.59	−34.29	−24.56

Table 3
Parameters obtained in the non-linear regression fitting of the experimental data of the adsorption isotherms at 25 °C onto the clay honeycomb monoliths.

Sample	I-S		ST	
Metal ions	Pb^{2+}	Cd^{2+}	Pb^{2+}	Cd^{2+}
Langmuir model				
Q_m	2.41	1.48	2.01	4.76
K_L	0.031	0.025	0.025	0.013
R^2_{adj}	0.988	0.999	0.983	0.997
χ^2	0.027	0.0004	0.060	0.011
SSE	0.028	0.0003	0.027	0.015
SD	0.097	0.010	0.095	0.071
BIC	−22.71	−45.38	−22.89	−25.83
Freundlich model				
n_F	2.53	2.29	2.24	1.76
K_F	0.290	0.138	0.177	0.188
R^2_{adj}	0.942	0.980	0.941	0.99
χ^2	0.125	0.030	0.157	0.069
SSE	0.135	0.016	0.093	0.057
SD	0.212	0.073	0.176	0.138
BIC	−14.84	−25.50	−16.7	−19.15
Redlich–Peterson model				
K_{RP}	0.051	0.037	0.041	0.071
a_{RP}	0.002	0.024	0.006	0.032
g	1.42	1.01	1.22	0.86
R^2_{adj}	0.999	0.999	0.982	0.997
χ^2	0.107	0.0004	0.044	0.012
SSE	0.114	0.0003	0.021	0.014
SD	0.238	0.012	0.102	0.078
BIC	−14.08	−43.80	−22.53	−24.56

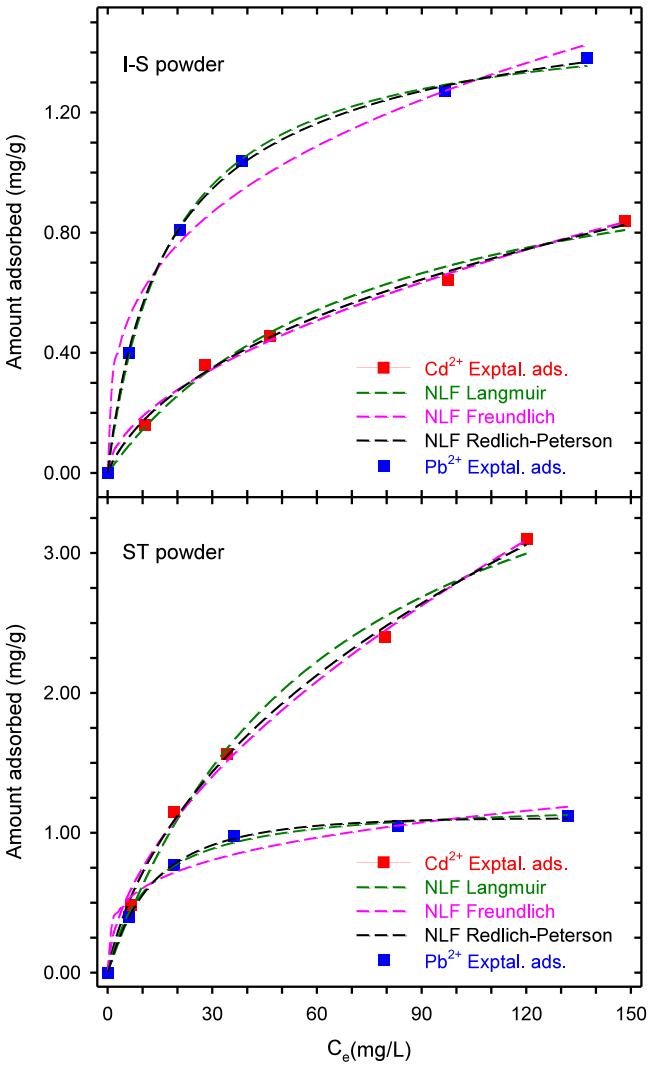

Fig. 10. Retention of Pb^{2+} and Cd^{2+} by the clays in the form of powder as function of the initial concentration: 2, 10, 30, 50, 100 and 150 ppm. pH: 4.5. Clay amount: 0.3 g of I-S and 0.4 g of ST. Contact time: 150 min. Non-linear fitting of the adsorption isotherms obtained for the clay powders to the Langmuir, Freundlich and Redlich–Peterson models is also included.

adsorption effect. In any case, comparison with results obtained by other authors should be always made with caution considering the diversity of experimental variables. For example, Padilla-Ortega et al. found very heterogeneous response when studying the binary adsorption of Cd^{2+}/Ni^{2+} on bentonite, Zn^{2+}/Cd^{2+} on sepiolite and Pb^{2+}/Cu^{2+} on vermiculite (Padilla-Ortega et al., 2013). He et al. observed high selectivity of Pb^{2+} during the competitive adsorption of Cd^{2+}, Pb^{2+} and Ni^{2+} onto Fe^{3+}-modified argillaceous limestone (He et al., 2018). Similarly, Djukić et al. reported selectivity effects for the simultaneous sorption of Ni, Cr, Cd and Pb ions on a natural montmorillonite (Djukić et al., 2013). In particular, almost complete (98%) sorption was achieved for Cr and Pb, while about 19% of the initial concentration of Cd and Ni persisted in the solution. On the other hand, Jiang et al. showed that the adsorption of Pb^{2+}, Cd^{2+}, Ni^{2+} and Cu^{2+} using kaolinite clay was not significantly different between single metal and multi-metal ions' competitive adsorption at a low initial concentration but the second type relatively decreased when initial metal ion concentration increased (Jiang et al., 2010).

There are other interesting previous studies in which the authors tried to understand the keys of the competition between lead and cadmium for the adsorption onto clayey substrates. For example, Oh et al. studied the competitive sorption of Pb and Cd onto a series of natural sediments finding a correlation with the CEC and BET surface area of the sediments (Oh et al., 2009). On this regard, Pokrovsky et al. did not observe competition between these two metals over acidic soils which was attributed to the fact that the surface sites remained far from being saturated (Pokrovsky et al.,

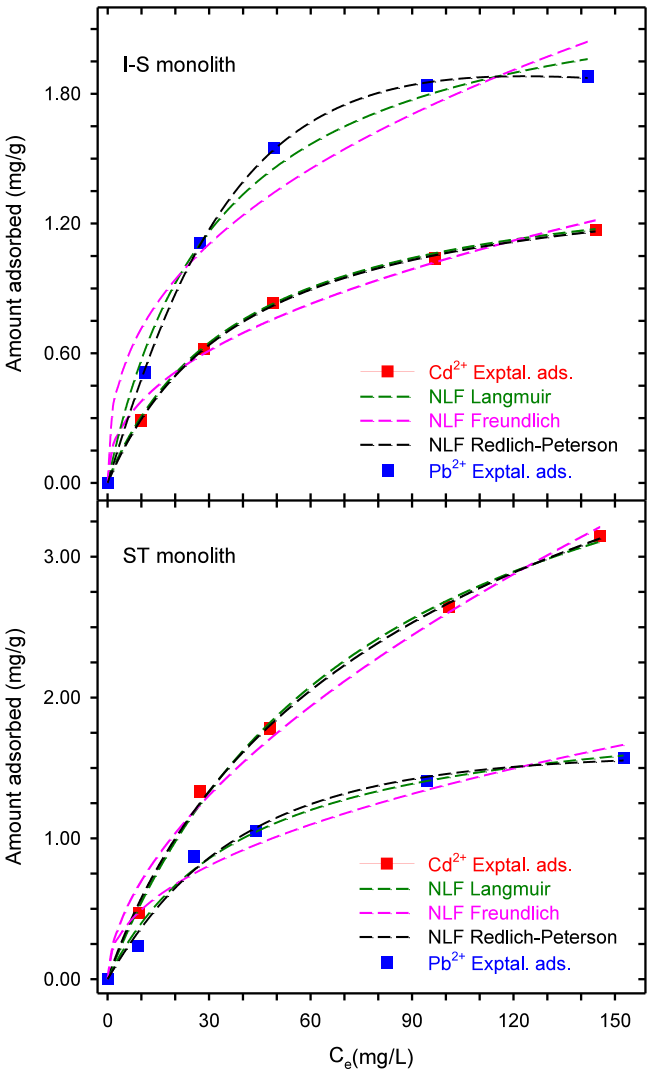

Fig. 11. Retention of Pb^{2+} and Cd^{2+} by the I-S and ST clays in the form of honeycomb monolith as function of the initial concentration: 2, 10, 30, 50, 100 and 150 ppm. pH: 4.5. Contact time: 150 min. Non-linear fitting of the adsorption isotherms obtained for the clay honeycomb monoliths to the Langmuir, Freundlich and Redlich–Peterson models is also included.

2012). In this sense, let us remind that our two investigated clays had relatively similar CEC values but one of them, the ST, showed clearly higher surface area than the other one, the I-S (Fig. 6). These data and the above cited references might explain that the illite–smectite is more affected by the coexistence of Pb^{2+} and Cd^{2+} in the aqueous solution (Fig. 12).

Finally, considering that the ST monolith exhibited the best response to the simultaneous presence of lead and cadmium as above commented, we selected this monolith to perform a complementary XRF analysis in multipoint mode after treatment with aqueous solution having 150 ppm of Pb^{2+} and 150 ppm of Cd^{2+} (Fig. 13). This analysis not only gave a direct evidence of the entrance of both heavy metals in the adsorbent but also showed their detection with relatively similar contents in the same analysed areas. This observation reinforces the idea of non-competitive adsorption under our experimental conditions above proposed.

4. Conclusions and implications

The study performed is a novel approach in the field of water contaminants removal by co-adsorption from Cd^{2+}/Pb^{2+} mixtures, still clearly dominated by powdered materials. In this work two natural Moroccan clays without further modification were employed. Before their use, a full physico-chemical characterization was performed. This study confirmed their mineralogical nature, illite–smectite and stevensite, standard properties regarding texture and cationic

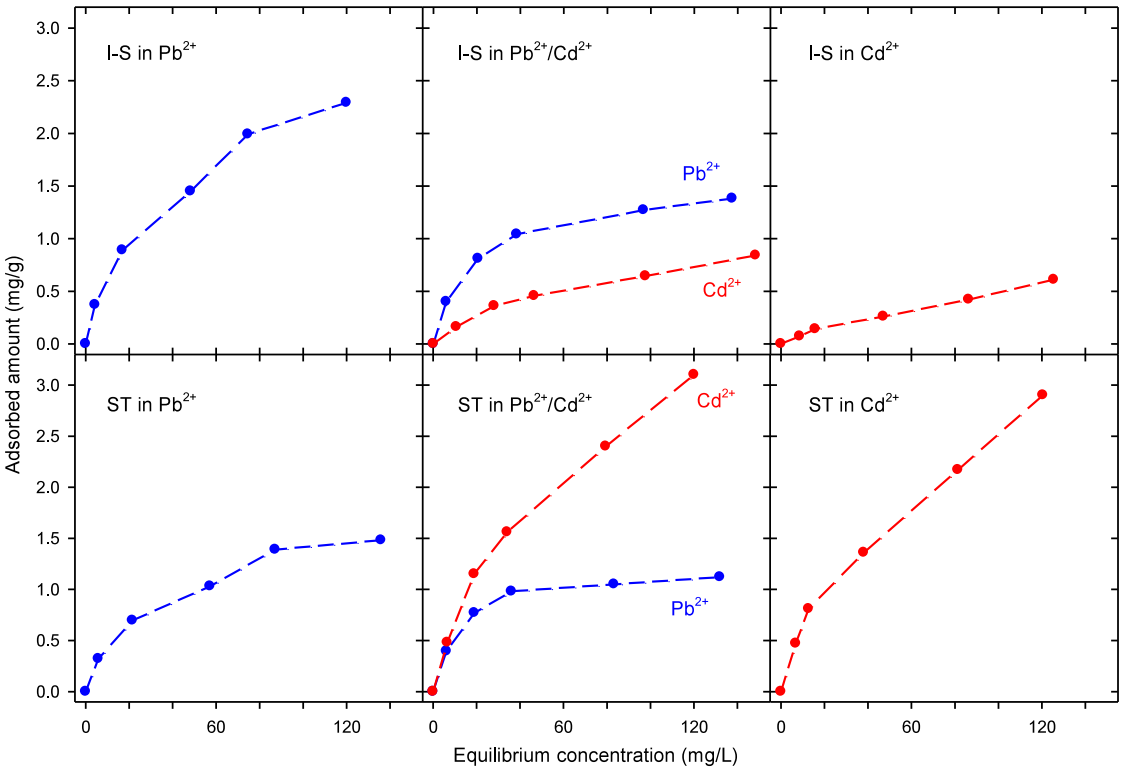

Fig. 12. Comparison between the performance of the clays in single and double solutions.

exchange capacity, easy extrudibility as honeycomb monoliths without additives, and good resistance of the structured filters to water after moderate calcination.

The adsorption tests, performed with both powders and honeycomb monoliths, revealed a pseudo-second order kinetics and good fitting to Redlich–Peterson model for both heavy metals. In addition, the total retention capacity of the stevensite was maintained in the bimetallic solution with respect to the scenario with the metals being separate, while it slightly diminished for the illite–smectite, most likely due to its lower specific surface area that implies more competition for the adsorption sites. In any case, and also remarkable, for both clays the coexistence of Pb^{2+} and Cd^{2+} ions in water favoured the adsorption of cadmium for both clays.

The results obtained with the honeycomb monoliths, which kept the powders efficiency, point out the potential of these clays for a use at great scale. The honeycomb design for the adsorbent adds the intrinsic advantages of a structured filter, among them easier handling and lower production of residues for the benefit of environment. Moreover, the combination of this design with the use of natural clays (cheap and abundant materials) in raw state opens up a promising alternative to higher cost technologies for water depollution, which can be of especial interest for developing countries.

CRediT authorship contribution statement

Mohammadi Ahrouch: Investigation. **José Manuel Gatica:** Conceptualization, Writing – review & editing, Supervision. **Khalid Draoui:** Funding acquisition, Supervision. **Dolores Bellido-Milla:** Methodology, Resources. **Hilario Vidal:** Conceptualization, Writing – original draft.

Declaration of competing interest

The authors declare that they have no known competing financial interests or personal relationships that could have appeared to influence the work reported in this paper.

Acknowledgements

The authors thank the Ministry of Economy and Competitiveness of Spain (Projects PID2020-113006-RB-I00 and PID2020-115843-RB-I00), the Junta de Andalucía, Spain (FQM-110 and FQM-249 groups, and Project P20-00918) and

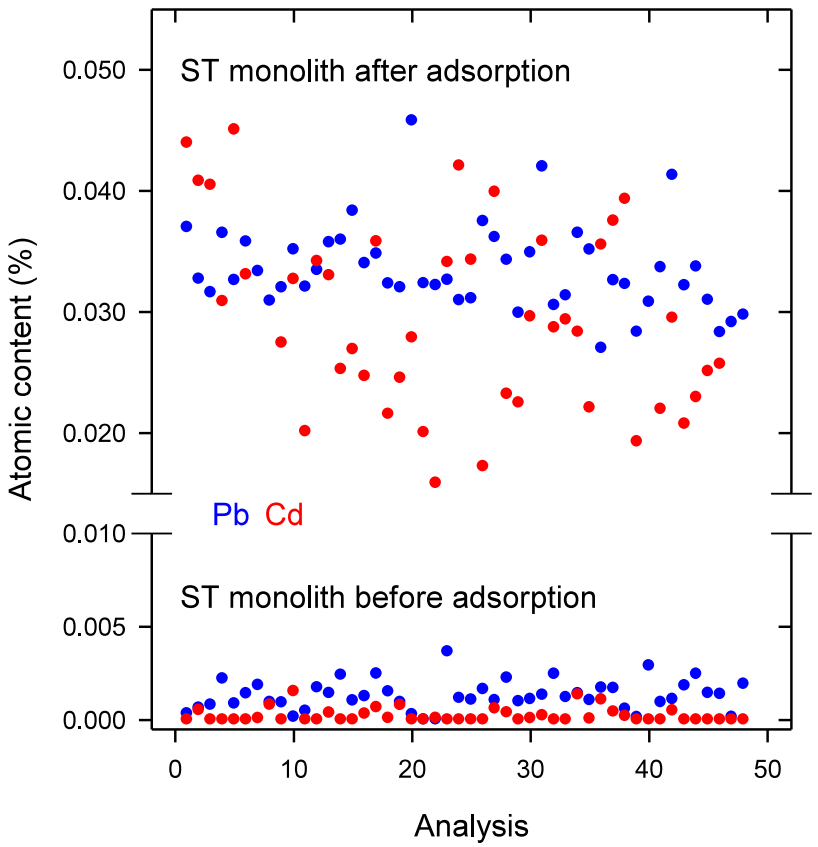

Fig. 13. Lead and cadmium content measured by XRF multipoint mode analysis over 1.5 mm × 0.5 mm rectangular zones of the ST clay honeycomb monolith after treatment for 150 min at pH 4.5 with water containing 150 ppm of Pb^{2+} and 150 ppm of Cd^{2+}. The analysis of the same monolith before the treatment is included as a reference.

the Institute of Electron Microscopy and Materials (IMEYMAT) of Cadiz University (UCA), Spain (Projects HOMOGREEN, NUPRECAT and BIOSENSEP) for their financial support. M. Ahrouch acknowledges the Aula Universitaria del Estrecho for a pre-doctoral grant. Thanks are also due to Dr. A.A. Lahcen from Cornell University (USA) and Dr. Y.A. El Haj Ali from Abdelmalek Essaadi University for their assistance in making the calculations for the non-linear fitting of the kinetic and equilibrium data.

References

Abdellaoui, Y., Olguín, M.T., Abatal, M., Ali, B., Díaz-Méndez, S.E., Santiago, A.A., 2019. Comparison of the divalent heavy metals (Pb, Cu, Cd) adsorption behavior by montmorillonite-KSF and their calcium- and sodium-forms. Superlattices Microstruct. 17, 165–175.

Abu-Danso, E., Peräniemi, S., Leivinskä, T., Kim, T., Tripathi, K.M., Bhatnagar, A., 2020. Synthesis of clay-cellulose biocomposite for the removal of toxic metal ions from aqueous medium. J. Hazard. Mater. 3181, 120871.

Adebowale, K., Unuabonah, I.E., Olu-Owalabi, B.I., 2006. The effect of some operating variables on the adsorption of lead and cadmium ions on kaolinite clay. J. Hazard. Mater. B 134, 130–139.

Ahrouch, M., Gatica, J.M., Draoui, K., Bellido, D., Vidal, H., 2019b. Lead removal from aqueous solution by means of integral natural clays honeycomb monoliths. J. Hazard. Mater. 365, 519–530.

Ahrouch, M., Gatica, J.M., Draoui, K., Bellido, D., Vidal, H., 2020. Honeycomb filters as an alternative to powders in the use of clays to remove cadmium from water. Chemosphere 259, 127526.

Ahrouch, M., Gatica, J.M., Draoui, K., Vidal, H., 2019a. Adding value to natural clays as low-cost adsorbents of methylene blue in polluted water through honeycomb monoliths manufacture. SN Appl. Sci. 1, 1595.

Ajala, M.A., Abdulkareem, A.S., Tijani, J.O., Kovo, A.S., 2022. Adsorptive behaviour of rutile phased titania nanoparticles supported on acid-modified kaolinite clay for the removal of selected heavy metal ions from mining wastewater. Appl. Water Sci. 12, 19.

Alyüz, B., Veli, S., 2009. Kinetics and equilibrium studies for the removal of nickel and zinc from aqueous solutions by ion exchange resins. J. Hazard. Mater. 167, 482–488.

Amalina, F., Syukor, A., Razak, A., Krishnan, S., A.W., Zularisam., Nasrullah, M., 2022. A comprehensive assessment of the method for producing biochar, its characterization, stability, and potential applications in regenerative economic sustainability – A review. Clean. Mater. 3, 100045.

Arif, M., Liu, G., Yousaf, B., Ahmed, R., Irshad, S., Ashraf, A., Zia-ur Rehman, M., Rashid, M.S., 2021. Synthesis, characteristics and mechanistic insight into the clays and clay minerals-biochar surface interactions for contaminants removal – A review. J. Clean. Prod. 310, 127548.

Ayari, F., E., Srasra., Trabelsi-Ayadi, M., 2005. Characterization of bentonitic clays and their use as adsorbent. Desalination 185, 391–397.

Aziz, F.F.A., Jalil, A.A., Hassan, N.S., Fauzi, A.A., Azami, M.S., Jusoh, N.W.C., Jusoh, R., 2022. A review on synergistic coexisting pollutants for efficient photocatalytic reaction in wastewater remediation. Environ. Res. 209, 112748.
Bailey, S.E., Olin, T.J., Bricka, R.M., Adrian, D.D., 1999. A review of potentially low-cost sorbents for heavy metals. Water Res. 33 (11), 2469–2479.
Baker, H.M., 2009. A study of the binding strength and thermodynamic aspects of cadmium and lead ions with natural silicate minerals in aqueous solutions. Desalination 242, 115–127.
Barakat, M.A., 2011. New trends in removing heavy metals from industrial wastewater. Arab. J. Chem. 4, 361–377.
Chabani, M., Amrane, A., Bensmaili, A., 2009. Equilibrium isotherms for nitrate on resin Amberlite IRA 400. J. Hazard. Mater. 165, 27–33.
Chafik, T., Harti, S., Cifredo, G., Gatica, J.M., Vidal, H., 2009. Easy extrusion of honeycomb-shaped monoliths using Moroccan natural clays and investigation of their dynamic adsorptive behaviour towards VOCs. J. Hazard. Mater. 170, 87–95.
Chen, G., Shi, L., 2017. Removal of Cd(II) and Pb(II) ions from natural water using a low-cost synthetic mineral: Behavior and mechanisms. RSC Adv. 69, 43445–43454.
Chen, P., Wang, Y., Zhuang, X., Liu, H., Liu, G., Lu, W., 2023. Selective removal of heavy metals by Zr-based MOFs in wastewater: new acid and amino functionalization strategy. J. Environ. Sci. 124, 268–280.
Cieseielski, H., Sterckeman, T., Santerne, M., Willery, J.P., 1997. Determination of cation exchange capacity and exchangeable cations in soils by means of cobalt hexamine trichloride, Effects of experimental conditions. Agronomie 17, 1–7.
Cifredo, G., Gatica, J.M., Harti, S., Vidal, H., 2010. Easy route to activate clay honeycomb monoliths for environmental applications. Appl. Clay Sci. 47, 392–399.
Cybulski, A., Moulijn, J.A., 1994. Monoliths in heterogeneous catalysis. Catal. Rev. 36 (2), 179–270.
De Gisi, S., Lofrano, G., Grassi, M., Notarnicola, M., 2016. Characteristics and adsorption capacities of low-cost sorbents for wastewater treatment: A review. Sustain. Mater. Technol. 9, 10–40.
Di, J., Ruan, Z., Zhang, S., Dong, Y., Fu, S., Li, H., Jiang, G., 2022. Adsorption mechanisms of Cu^{2+}, Zn^{2+} and Pb^{2+} by magnetically modified lignite. Sci. Rep. 12, 1394.
Djukić, A., Jovanović, U., Tuvić, T., Andrić, V., Novaković, J.G., Ivanović, N., Matović, L., 2013. The potential of ball-milled Serbian natural clay for removal of heavy metal contaminants from wastewaters: simultaneous sorption of Ni, Cr, Cd and Pb ions. Ceram. Int. 39, 7173–7178.
El-Korashy, S.A., Elwakeel, K.Z., El-Hafeiz, A.A., 2016. Fabrication of bentonite/thiourea-formaldehyde composite material for Pb(II), Mn(VII) and Cr(VI) sorption: A combined basic study and industrial application. J. Clean. Prod. 137, 40–50.
Elwakeela, K.Z., El-Bindary, A.A., Kouta, E.Y., 2017. Retention of copper, cadmium and lead from water by Na-Y-Zeolite confined in methyl methacrylate shell. J. Environ. Chem. Eng. 5, 3698–3710.
Femina Carolin, C., Senthil Kumar, P., Saravanan, A., Janet Joshiba, G., Naushad, M., 2017. Efficient techniques for the removal of toxic heavy metals from aquatic environment: A review. J. Environ. Chem. Eng. 5, 2782–2799.
Fu, F., Wang, Q., 2011. Removal of heavy metal ions from wastewaters: A review. J. Environ. Manage. 42, 407–418.
Gang, D., Ahmad, Z.U., Lian, Q., Yao, L., Zappi, M.E., 2021. A review of adsorptive remediation of environmental pollutants from aqueous phase by ordered mesoporous carbon. Chem. Eng. J. 403, 126386.
García-Carvajal, C., Villarroel-Rocha, J., Curvale, D., Barroso, M.M., Sapag, K., 2019. Arsenic (V) removal from aqueous solutions using natural clay ceramic monoliths. Chem. Eng. Commun. 206, 1440–1451.
Gatica, J.M., Gómez, D.M., S., Harti., Vidal, H., 2013. Clay honeycomb monoliths for water purification: modulating methylene blue adsorption through controlled activation via natural coal templating. Appl. Surf. Sci. 277, 242–248.
Gatica, J.M., Rodríguez-Izquierdo, J.M., Sánchez, D., Ania, C., Parra, J.B., Vidal, H., 2004. Extension of preparation methods employed with ceramic materials to carbon honeycomb monoliths. Carbon 42, 3251–3254.
Gatica, J.M., Vidal, H., 2011. Use of clays to manufacture honeycomb monoliths for pollution control applications. In: Humphrey, J.P., Boyd, D.E. (Eds.), Clay: Types, Properties and Uses. Nova Science Publishers Inc, New York, pp. 253–273.
Gode, F., Pehlivan, E., 2006. Removal of chromium (III) from aqueous solutions using lewatit s 100: the effect of pH, time, metal concentration and temperature. J. Hazard. Mater. 136, 330–337.
Harti, S., Cifredo, G., Gatica, J.M., Vidal, H., Chafik, T., 2007. Physicochemical characterization and adsorptive properties of some Moroccan clay minerals extruded as lab-scale monoliths. Appl. Clay Sci. 36, 287–296.
He, S., Li, Y., Weng, L., Wang, J., He, J., Liu, Y., Zhang, K., Wu, Q., Zhang, Y., Zhang, Z., 2018. Competitive adsorption of cd^{2+}, pb^{2+} and Ni^{2+} onto fe^{3+}-modified argillaceous limestone: influence of pH, ionic, strength and natural organic matters. Sci. Total Environ. 617-618, 69–78.
Humphrey, J.P., Boyd, D.E., 2011. Clay: Types, Properties and Uses. Nova Science Publishers, New York.
Jiang, M.Q., Jin, X.Y., Lu, X.Q., Chen, Z.L., 2010. Adsorption of Pb(II), Cd(II), Ni(II) and Cu(II) onto natural kaolinite clay. Desalination 252, 33–39.
Joseph, L., Jun, B.-M., Flora, J.R.V., Park, C.M., Yoon, Y., 2019. Removal of heavy metals from water sources in the developing world using low-cost materials: A review. Chemosphere 229, 142–159.
Jusoh, A., Shiung, L.S., Ali, N., Noor, M.J.M.M., 2007. A simulation study of the removal efficiency of granular activated carbon on cadmium and lead. Desalination 206, 9–16.
Kang, K.C., Kim, S.S., Choi, J.W., Kwon, S.H., 2008. Sorption of cu^{2+} and cd^{2+} onto acid- and base-pretreated granular activated carbon and activated carbon fiber samples. J. Ind. Eng. Chem. 14 (1), 131–135.
Khalfa, L., Sdiri, A., Bagane, M., Cervera, M.L., 2021. A calcined clay fixed bed adsorption studies for the removal of heavy metals from aqueous solutions. J. Clean. Prod. 278, 123935.
Kumar, V., Dwivedi, S.K., Oh, S., 2022. A review on microbial-integrated techniques as promising cleaner option for removal of Cr, Cd and Pb from industrial wastewater. J. Water Process. Eng. 47, 102727.
Lee, S., Choi, H., 2018. Persimmon leaf bio-waste for adsorptive removal of heavy metals from aqueous solution. J. Environ. Manage. 209, 382–392.
Liu, F., Li, I., Ling, P., Jing, X., Li, C., Li, A., You, X., 2011. Interaction mechanism of aqueous heavy metals onto a newly synthesized IDA-chelating resin: isotherms, thermodynamics and kinetics. Chem. Eng. J. 173, 106–114.
Mnasri-Ghnimi, S., Frini-Srasra, N., 2019. Removal of heavy metals from aqueous solutions by adsorption using single and mixed pillared clays. Appl. Clay Sci. 179, 105151.
Motsi, T., Rowson, N.A., Simmons, M.J.H., 2009. Adsorption of heavy metals from acid mine drainage by natural zeolite. Int. J. Miner. Process. 92, 42–48.
Nagy, B., Mânzatu, C., Măicăneanu, A., Indolean, C., Lucian, B.-T., Majdik, C., 2017. Linear and nonlinear regression analysis for heavy metals removal using *Agaricus bisporus* macrofungus. Arab. J. Chem. 10, S3569–S3579.
Novikau, R., Lujaniene, G., 2022. Adsorption behaviour of pollutants: Heavy metals, radionuclides, organic pollutants, on clays and their minerals (raw, modified and treated): A review. J. Environ. Manage. 309, 114685.
Oh, S., Kwak, M.Y., Shin, W.S., 2009. Competitive sorption of lead and cadmium onto sediments. Chem. Eng. J. 152, 376–388.
Ostroski, I.C., Barros, M.A.S.D., Silva, E.A., Dantas, J.H., Arroyo, P.A., Lima, O.C.M., 2009. A comparative study for the ion exchange of Fe(III) and Zn(II) on zeolite NaY. J. Hazard. Mater. 161, 1404–1412.
Otunola, B.O., Ololade, O.O., 2020. A review on the application of clay minerals as heavy metal adsorbents for remediation purposes. Environ. Technol. Innov. 18, 100692.

Padilla-Ortega, E., Leyva-Ramos, R., Flores-Cano, J.V., 2013. Binary adsorption of heavy metals from aqueous solution onto natural clays. Chem. Eng. J. 225, 535–546.
Parveen, S., Bhat, I.U.H., Khanam, Z., Rak, A.E., Yusoff, H.M., Akhter, M.S., 2022. Phytoremediation: In situ alternative for pollutant removal from contaminated natural media: a brief review. Biointerf. Res. Appl. Chem. 12 (4), 4945–4960.
Pokrovsky, O.S., Probst, A., Leviel, E., Liao, B., 2012. Interactions between cadmium and lead with acidic soils: experimental evidence of similar adsorption patterns for a wide range of metal concentrations and the implications of metal migration. J. Hazard. Mater. 199–200, 358–366.
Sajidu, S.M.I., Persson, I., Masamba, W.R.I., Henry, E.M.T., 2008. Mechanisms of heavy metal sorption on alkaline clays from Tundulu in Malawi as determined by EXAFS. J. Hazard. Mater. 158, 401–409.
Sanchooli, M., Rahdar, S., Taghavi, M., 2016. Cadmium removal from aqueous solutions using saxaul tree ash. Iran J. Chem. Eng. 35 (3), 45–52.
Sellaoui, L., Soetaredjo, F.E., Ismadji, S., Bonilla-Petriciolet, A., Belver, C., Bedia, J., Lamine, A.B., Erto, A., 2018. Insights on the statistical physics modelling of the adsorption of Cd^{2+} and Pb^{2+} ions on bentonite-chitosan composite in single and binary systems. Chem. Eng. J. 354, 569–576.
Sharma, V., Borkute, G., Gumfekar, S.P., 2022. Biomimetic nanofiltration membranes: critical review of materials, structures, and applications to water purification. Chem. Eng. J. 433, 133823.
Siddiqui, S.H., 2018. The removal of Cu^{2+}, Ni^{2+} and methylene blue (MB) from aqueous solution using Luffa Actangula carbon: kinetics, thermodynamic and isotherm and response methodology. Growndwater Sustain. Dev. 6, 141–149.
Singh, A., Chauan, S., Varjani, S., Pandey, A., Bhargava, P.C., 2022. Integrated approaches to mitigate threats from emerging potentially toxic elements: a way forward for sustainable environmental management. Environ. Res. 209, 112844.
Spiess, A.-N., Neumeyer, N., 2010. An evaluation of R^2 as an inadequate measure for nonlinear models in pharmacological and biochemical research: a Monte Carlo approach. BMC Pharmacol. 10 (6).
Taffarel, S.R., Rubio, J., 2009. On the removal of Mn^{2+} ions by adsorption onto natural and activated Chilean zeolites. Miner. Eng. 22, 336–343.
Thommes, M., Kaneko, K., Neimark, A.V., Olivier, J.P., Rodriguez-Reinoso, F., Rouquerol, J., Sing, K.S.W., 2015. Physisorption of gases, with special reference to the evaluation of surface area and pore size distribution (IUPAC Technical Report). Pure Appl. Chem. 87 (9–10), 1051–1069.
Tran, H.N., You, S.-J., Hosseini-Bandegharaei, A., Chao, H.-P., 2017. Mistakes and inconsistencies regarding adsorption of contaminants from aqueous solutions: a critical review. Water Res. 120, 88–116.
Uddin, M.K., 2017. A review on the adsorption of heavy metals by clay minerals, with special focus on the past decade. Chem. Eng. J. 308, 438–462.
Vhahangwele, M., Mugera, G.W., 2015. The potential of ball-milled South African bentonite clay for attenuation of heavy metals from acidic wastewaters: simultaneous sorption of Co^{2+}, Cu^{2+}, Ni^{2+}, Pb^{2+}, and Zn^{2+} ions. J. Environ. Chem. Eng. 3, 2416–2425.
Vidal, H., Rubido, M., Yeste, M.P., Cifredo, G.A., Gatica, J.M., 2016. Natural clays for CO_2 sequestration: study in the form of powder as previous stage before their use in structured filters. Int. J. Latest Res. Eng. Technol. 2 (11), 6–14.
Zhang, Q., Cheng, Y.-F., Huang, B.-C., Jin, R.-C., 2022. A review of heavy metals inhibitory effects in the process of anaerobic ammonium oxidation. J. Hazard. Mater. 429, 128362.
Zhang, T., Wang, W., Zhao, Y., Bai, H., Wen, T., Kang, S., Song, G., Song, S., Komarneni, S., 2021. Removal of heavy metals and dyes by clay-based adsorbents: From natural clays to 1D and 2D nano-composites. Chem. Eng. J. 420, 127574.
Zhu, D., He, Y., Zhang, B., Zhang, N., Lei, Z., Zhang, Z., Chen, G., Shmizu, K., 2021. Simultaneous removal of multiple heavy metals from wastewater by novel plateau laterite ceramic in batch and fixed-bed studies. J. Environ. Chem. Eng. 9, 105792.